Astron. Astrophys. 154, 231–242 (1986)

ASTRONOMY AND ASTROPHYSICS

Structure and merging of solar magnetic fluxtubes

G.W. Pneuman[1,2], S.K. Solanki[1], and J.O. Stenflo[1]

[1] Institute of Astronomy, ETH-Zentrum, CH-8092 Zurich, Switzerland
[2] High Altitude Observatory, National Center for Atmospheric Research, Boulder, CO, USA

Received April 23, accepted July 9, 1985

Summary. An expansion technique is employed to derive a model of magnetic fluxtubes in the solar atmosphere which takes into account the effects of field line curvature, internal structural variations, and the merging of the tube with its immediate neighbours as it expands. The merging is accomplished by the use of a small 'seed' magnetic field between the tubes which, in the limit of vanishing strength, has no influence on the solution. For conditions where the internal temperature of an untwisted tube is taken to be the same as that outside, the fluxtube properties are independent of the magnetic field strength at the base and depend only on the initial diameter and filling factor. For a fixed filling factor, the merging height is almost a linearly increasing function of base diameter whereas, for a fixed base diameter, the merging height increases as the filling factor decreases. For filling factors of about 0.1 or less, the merging is predicted to take place in the chromosphere. For unequal internal and external temperatures, the merging height does depend upon field strength and increases with increasing field strength if the tube is hotter than its surroundings and vice versa if it is cooler.

For our solutions, the internal magnetic structure of the tube evolves in height in a decidedly non-self-similar manner. However, for the special case when the internal temperature is both uniform and equal to the external temperature, the gas pressure can vary self-similarly. The axial magnetic field declines outward from the axis if the base gas pressure is either uniform or increasing outward, but may initially increases outward if the pressure declines. In the vicinity of the merging height, the field approaches uniformity consistent with a vertical tube with constant cross-section. For twisted tubes the number of turns per unit length along the tube remains approximately constant, so that the pitch angle of the field increases rapidly with height as the tube expands. It then reaches a maximum and decreases to a constant asymptotic value when merging takes place.

Key Words: Fluxtubes – magnetic fields – hydromagnetics – faculae

1. Introduction

It is now well established that the solar magnetic field outside sunspots below chromospheric levels is not uniformly distributed, but concentrated into discrete fluxtubes (Howard and Stenflo, 1972) where the field strength is about 1000–2000 G (Stenflo, 1973; Harvey, 1977). The structure is determined by a force balance between the magnetic field and gas pressure inside the tube with the gas pressure outside. Since this external gas pressure declines upward rapidly, the fluxtube must then expand with height in an appropriate manner in order to maintain equilibrium with its surroundings.

Theoretical modeling of thin fluxtubes has received an increasing amount of attention. The first crude models employed the so-called "thin fluxtube approximation" where the internal magnetic field is assumed to be purely axial and uniform across the cross-section (cf. Defouw, 1976; Roberts and Webb, 1978; Unno and Ribes, 1979: Meyer et al., 1979; Spruit, 1981). In these models, all other quantities such as pressure, temperature, etc. are also taken to be uniform. Potential field models of small fluxtubes have been constructed by Spruit (1976) and Simon et al. (1983), and models employing the similarity approximation, introduced by Schlüter and Temesvary (1958), have been developed by Wilson (1977a,b), Solanki (1982), and Osherovich et al. (1983). Finally, Deinzer et al. (1984a,b) have recently published fully self-consistent MHD models using a two dimensional slab geometry.

Since the fluxtubes, if unobstructed, would expand indefinitely with height, we expect that any discrete set of tubes would eventually merge together at some height and coalesce into larger field distributions. It is this effect we wish to study in some detail in this paper and we hope to be able to elucidate the dependence of the merging properties of fluxtube collections upon various relevent parameters such as filling factor, tube radius, magnetic field strength, etc. Others (Gabriel, 1976; Anzer and Galloway, 1983a,b) have considered a similar problem for entire network and active regions using the potential field approximation. We wish here to relax this assumption and study the phenomenon from the MHD standpoint and also to study small individual fluxtubes instead of the network or active region as a whole. We desire a model which possesses internal structure as opposed to the thin fluxtube models, but still not constrain ourselves to similarity theory. Similarity models force the field to have the same form at all heights. This is incompatible with the merging of fluxtubes, as we shall see in Sect. 3. They also place a constraint on the temperature variation across the tube. This seems somewhat artificial since no energy equation is used. We shall return to this point later.

The approach we will use here is to expand the MHD equations in a power series about the tube axis so that the thin fluxtube approximation is the zeroth order solution and higher terms

Send offprint requests to: S.K. Solanki

represent corrections to this introduced by finite width. A similar expansion approach has been recently suggested by Browning and Priest (1984). Because our model will give two-dimensional information on fluxtube structure and because, unlike similarity models, we can consider arbitrary temperature distributions or incorporate an energy equation, we hope that it could serve as a basis for future two-dimensional empirical models. For such work it has the advantage of being relatively simple and easy to compute compared to a completely self-consistent treatment, based for example on a relaxation technique (Deinzer et al., 1984a,b) or on the method of Pneuman and Kopp (1971). Here, it is relatively simple to separate out various interacting effects and assess their relative importance.

2. Basic method and equations

Consider a model vertical fluxtube as shown in Fig. 1. r, θ, and z are ordinary cylindrical coordinates and the tube is assumed rotationally symmetric about the z axis. We define the reference values for the axial field strength, gas pressure, temperature and other quantities at a reference level $z = 0$ and at the tube axis $r = 0$ as B^*, P^*, T^* etc. respectively. R^* denotes the tube radius at $z = 0$. The radius of the tube is $R(z)$. In this coordinate system, the force balance in the three coordinate directions plus the expression $\nabla \cdot \mathbf{B} = 0$ yield

$$4\pi \frac{\partial P}{\partial r} = B_z\left(\frac{\partial B_r}{\partial z} - \frac{\partial B_z}{\partial r}\right) - \frac{B_\theta}{r}\frac{\partial}{\partial r}(rB_\theta) \tag{1}$$

$$0 = \frac{B_r}{r}\frac{\partial}{\partial r}(rB_\theta) + B_z\frac{\partial B_\theta}{\partial z} \tag{2}$$

$$4\pi\left(\frac{\partial P}{\partial z} + \frac{P}{H}\right) = -Br\left(\frac{\partial B_r}{\partial z} - \frac{\partial B_z}{\partial r}\right) - B_\theta\frac{\partial B_\theta}{\partial z} \tag{3}$$

$$0 = \frac{1}{r}\frac{\partial}{\partial r}(rB_r) + \frac{\partial B_z}{\partial z} \tag{4}$$

where P is the gas pressure, B_r, B_θ, and B_z the three compontents of the magnetic field, and H the scale height defined by

$$H(z) = \frac{kT(z)R_\odot^2}{Gm_pM_\odot}$$

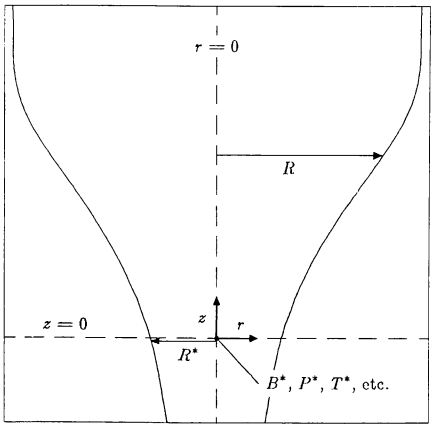

Fig. 1. Schematic of fluxtube geometry showing pertinent definitions

k being Boltzmann's constant, T the temperature, $R_\odot$ the solar radius, G the gravitational constant, m_p the mean particle mass, and $M_\odot$ the solar mass. We now put Eqs. (1)–(4) in nondimensional from by defining $x = r/H^*$, $y = z/H^*$, $\mathbf{b} = \mathbf{B}/B^*$, $p = P/P^*$ and $\sigma = T/T^*$ to obtain

$$\beta\frac{\partial p}{\partial x} = b_z\left(\frac{\partial b_r}{\partial y} - \frac{\partial b_z}{\partial x}\right) - \frac{b_\theta}{x}\frac{\partial}{\partial x}(xb_\theta) \tag{5}$$

$$0 = \frac{b_r}{x}\frac{\partial}{\partial x}(xb_\theta) + b_z\frac{\partial b_\theta}{\partial y} \tag{6}$$

$$\beta\left(\frac{\partial p}{\partial y} + \frac{p}{\sigma}\right) = -b_r\left(\frac{\partial b_r}{\partial y} - \frac{\partial b_z}{\partial x}\right) - b_\theta\frac{\partial b_\theta}{\partial y} \tag{7}$$

$$0 = \frac{1}{x}\frac{\partial}{\partial x}(xb_r) + \frac{\partial b_z}{\partial y} \tag{8}$$

where $H^* = kT^*R_\odot^2/(Gm_pM_\odot)$ and $\beta = 4\pi P^*/B^{*2}$.

We now expand all variables in a power series in x. As for the case of potential fields as well as analytic force-free fields (cf. Ferraro and Plumpton, 1966), we express b_z as an even series in x and b_r, b_θ as odd series, i.e.,

$$b_z = h_0 + h_2x^2 + h_4x^4 + \cdots$$

$$b_r = f_1x + f_3x^3 + \cdots$$

$$b_\theta = g_1x + g_3x^3 + \cdots$$

The form of the Eqs. (5)–(8) suggests that p and σ are also even.[1]

$$p = p_0 + p_2x^2 + p_4x^4 + \cdots$$

$$\sigma = \sigma_0 + \sigma_2x^2 + \sigma_4x^4 + \cdots$$

Now Eqs. (5)–(8) assume the form

$$\begin{aligned}2\beta(p_2 + 2p_4x^2 + \cdots) &= (h_0 + h_2x^2 + \cdots)((f_1' + f_3'x^2 + \cdots) - (2h_2 + 4h_4x^2 + \cdots)) \\ &\quad - (g_1 + g_3x^2 + \cdots)(2g_1 + 4g_3x^2 + \cdots)\end{aligned} \tag{9}$$

$$\begin{aligned}0 &= 2(f_1 + f_3x^2 + \cdots)(g_1 + 2g_3x^2 + \cdots) \\ &\quad + (h_0 + h_2x^2 + \cdots)(g_1' + g_3'x^2 + \cdots)\end{aligned} \tag{10}$$

$$\begin{aligned}&\beta((\sigma_0 + \sigma_2x^2 + \cdots)(p_0' + p_2'x^2 + \cdots) + (p_0 + p_2x^2 + \cdots)) \\ &= (\sigma_0 + \sigma_2x^2 + \cdots)(-(f_1x + f_3x^3 + \cdots)((f_1'x + f_3'x^3 + \cdots) \\ &\quad -(2h_2x + h_4x^3 + \cdots)) - (g_1x + g_3x^3 + \cdots)(g_1'x + g_3'x^3))\end{aligned} \tag{11}$$

$$0 = (2f_1 + 4f_3x^2 + \cdots) + (h_0' + h_2'x^2 + \cdots) \tag{12}$$

where the prime denotes differentiation with respect to y. Equating equal powers of x up through terms of $O(x^2)$ yields

x^0 terms:

$$\sigma_0p_0' + p_0 = 0 \tag{13}$$

$$h_0(f_1' - 2h_2) - 2g_1^2 = 2\beta p_2 \tag{14}$$

$$2f_1g_1 + h_0g_1' = 0 \tag{15}$$

$$2f_1 + h_0' = 0 \tag{16}$$

[1] It can be shown that this form of expansion for b, p, and σ is the only one that leads to a solvable system of equations for finding successively higher order terms

x^2 terms:

$$\beta(\sigma_0 p_2' + \sigma_2 p_0' + p_2) = -\sigma_0 f_1(f_1' - 2h_2) \tag{17}$$

$$h_0(f_3' - 4h_4) + h_2(f_1' - 2h_2) - 6g_1 g_3 = 4\beta p_4 \tag{18}$$

$$4f_1 g_3 + 2g_1 f_3 + h_0 g_3' + h_2 g_1' = 0 \tag{19}$$

$$4f_3 + h_2' = 0 \tag{20}$$

Since we are considering a fluxtube with a discrete boundary, we must also satisfy two additional equations – that for the continuity of $P + B^2/8\pi$ and the conservation of total axial magnetic flux, i.e.,

$$(2\beta p + b^2)|_{x=a} = \Phi$$

$$\int_0^a b_z x\, dx = \text{const.}$$

where $\Phi = (8\pi P_e + B_e^2)/B^{*2}$, P_e and B_e being the external gas pressure and magnetic field strength respectively, and $a = R/H^*$. As before, we also expand the above two equations in powers of x up through terms of order x^2 (actually a^2 here) to obtain

$$(2\beta p_0 + h_0^2) + a^2(2\beta p_2 + f_1^2 + g_1^2 + 2h_0 h_2) = \Phi \tag{21}$$

$$h_0 a^2 = a^{*2} \tag{22}$$

where $a^* = R^*/H^*$. In the above, we have now introduced the additional unknown $a(y)$. If we were to append an energy equation to the system, the temperature would also be a variable unknown. However, we will not attempt this here and, therefore, have the liberty to arbitrarily specify σ_0 and σ_2. In similarity solutions, constraints are put upon the temperature in order to satisfy force balance and, hence, an energy equation in general cannot be satisfied. Here, we are not encumbered by this problem.

Equations (13)–(22) represent 10 equations in the 11 unknowns p_0, p_2, p_4, h_0, h_2, h_4, f_1, f_3, g_1, g_3, and a. Note, however, that Eq. (18) expresses only a relationship between p_4 and h_4, which appear nowhere else in the system. Hence, if we omit Eq. (18), we have 9 equations in 9 unknowns and a closed system. If one wished to find p_4 and h_4 explicitly, the x^4 term of Eq. (9), i.e.,

$$\begin{aligned}\beta(\sigma p_4' + p_4 + \sigma_2 p_2' + \sigma_4 p_0') &= -\sigma_0(f_1 f_3' - f_3 f_1' + 4f_1 h_4 + 2f_3 h_2) \\ &\quad -\sigma_2(f_1 f_1' - 2f_1 h_2) - \sigma_0(g_1 g_3' + g_3 g_1') - \sigma_2 g_1 g_1'\end{aligned} \tag{23}$$

could be used along with Eq. (18) to solve for these quantities in terms of the others which are known. We actually will do this later to check the smallness of p_4 and h_4 and, hence the validity of our solution.

We can now use Eqs. (13)–(17) and (22) to write p_0, f_1, g_1, p_2, h_2, and a in terms of h_0 and the temperature.

$$p_0 = \exp\left(-\int_0^y \frac{dy}{\sigma_0}\right) \tag{24}$$

$$f_1 = -\frac{h_0'}{2} \tag{25}$$

$$g_1 = g_1^* h_0 \tag{26}$$

$$p_2 = h_0\left(p_2^* + \int_0^y \frac{\sigma_2}{\sigma_0^2 h_0}\, dy\right)\exp\left(-\int_0^y \frac{dy}{\sigma_0}\right) \tag{27}$$

$$h_2 = -\frac{1}{4}h_0'' - g_1^{*2} h_0 - \beta\left(p_2^* + \int_0^y \frac{\sigma_2}{\sigma_0^2 h_0}\, dy\right)\exp\left(-\int_0^y \frac{dy}{\sigma_0}\right) \tag{28}$$

$$a = \frac{a^*}{\sqrt{h_0}} \tag{29}$$

Consider now a collection of vertical cylindrically symmetric fluxtubes which, at the level $y = 0$, occupy a certain fraction of the area given by a filling factor α. Since our model has a well defined and sharp boundary there is no ambiguity in the definition of α. As these fluxtubes each expand individually with height, they will eventually merge with each other when their areas (assuming they are all equal) have increased by the fraction $1/\alpha$. Actually, when these tubes begin to merge, the assumption of cylindrical symmetry will break down since there is no way to fill all space with a collection of cylinders. However, by this time the internal fields will have become vertical and uniform anyway, so the assumption of cylindrical symmetry is really not necessary. This is not true for twisted fields, and these shall be discussed separately (see Sect. 3.3).

In order to obtain smooth merging it is convenient to use a small seed magnetic field external to the tubes to simulate the presence of the neighbouring fluxtubes. This seed field is used only for convenience and in no way restricts the scope of our study since, if this field is sufficiently small at the reference level, all properties of the solution such as tube shape, merging height, etc. are independent of the strength of the seed field. Moreover, the use of this small external field might even be physically quite realistic since we hardly expect the magnetic field strength between the fluxtubes to be *identically* zero. If the magnitude of the seed field is B_e and it fills all available space between fluxtubes, then the conservation of flux yields

$$B_e = B_e^* h_0\left(\frac{1-\alpha}{h_0 - \alpha}\right)$$

where B_e^* is the value of B_e at $y = 0$. This relation for B_e clearly shows that as the fluxtube expands and the value of h_0 approaches α, B_e becomes large, mimicking the effect of a neighbouring fluxtube by forcing the model tube to become straight. We now substitute Eqs. (24) to (29) into Eq. (21) to obtain

$$\begin{aligned}h_0'' - \frac{1}{2h_0}(h_0')^2 = \frac{2}{a^{*2}}\Bigg(h_0^2\left(1 - \frac{\mu}{h_0}\right) + 2\beta p_0 \\ - \frac{1}{B^{*2}}\left(8\pi P_e + B_e^{*2} h_0^2\left(\frac{1-\alpha}{h_0 - \alpha}\right)^2\right)\Bigg).\end{aligned} \tag{30}$$

where $\mu = a^{*2} g_1^{*2}$.[2] Similarly Eqs. (18) and (19) can be used to write f_3 and g_3 in terms of h_0 and h_2.

$$f_3 = -\frac{1}{4}h_2' \tag{31}$$

$$g_3 = h_0^2\left(g_3^* - \frac{g_1^*}{2}\int_0^y \frac{1}{h_0^3}(h_2' h_0 - 2h_2 h_0')\, dy\right) \tag{32}$$

If needed f_3 and g_3 can easily be rewritten in terms of h_0 alone, but the resulting expressions are pondersome and offer no new insight.

[2] For the case when $h_2 = g_3 = 0$, $\mu = \tan^2\eta$ where η is the pitch angle at $R = R^*$

An examination of Eq. (30) without the seed field and for $\mu = 0$ shows that the right-hand-side, if set to zero, is just the thin fluxtube approximation for a uniform B_z field. The left-hand-side represents the contributions due to the radial field and to curvature. One interesting question we can ask at this point is – How important are these corrections to the slender fluxtube equations likely to be? We can estimate this by solving Eq. (30) without the left-hand-side (slender fluxtube equation) calculating the left-hand-side from that solution, and comparing it to the first term on the right-hand-side. Neglecting twist and the external field for the moment, we write Eq. (30) in the form

$$h_0'' - \frac{1}{2h_0}(h_0')^2 - \frac{2h_0^2}{a^{*2}} = -Q(y) \tag{33}$$

where

$$Q(y) = \frac{2}{a^{*2}}\left(\frac{8\pi P_e}{B^{*2}} + \beta \exp\left(-\int_0^y \frac{dy}{\sigma_0}\right)\right).$$

From the slender fluxtube approximation we have

$$h_0 = \frac{a^*}{\sqrt{2}} Q^{1/2}$$

$$h_0' = \frac{a^*}{2\sqrt{2}} Q^{-1/2} Q'$$

$$h_0'' = \frac{a^*}{2\sqrt{2}}\left(Q^{-1/2}Q'' - \frac{1}{2}Q^{-3/2}(Q')^2\right)$$

For simplicity, let us neglect the internal gas pressure ($\beta \approx 0$). Then

$$Q = \frac{16\pi P_e}{a^{*2}B^{*2}}.$$

If we now let the external gas pressure decline upwards exponentially, i.e.

$$P_e = P_e^* e^{-z/H_e},$$

where H_e is the scale height and

$$P_e^* = \frac{B^{*2}}{8\pi},$$

then

$$Q = \frac{2}{a^{*2}} e^{-z/H_e}$$

and the ratio, R_a, of the correction terms $h_0'' - \frac{1}{2h_0}(h_0')^2$ to the slender fluxtube term $2a^{*2}/h_0^2$ is just

$$R_a = \frac{a^*}{2\sqrt{2}Q^{5/2}}\left(QQ'' - \frac{3}{4}(Q')^2\right) = \frac{1}{16}\left(\frac{R^*}{H_e}\right)^2 \exp\left(\frac{z}{2H_e}\right)$$

Thus, even though the initial radius of the tube may be small as compared to the scale height, the correction terms will always eventually become important over distances of the order of a few scale heights. This, of course, is due to the rapid broadening of the tube with height.

As the individual fluxtubes expand upward, we will consider them merged when the quantity h_0'/h_0 becomes less than some small arbitrary value. Not far above this height the internal field becomes uniform ($h_2 \to 0$) and h_0 approaches the constant value

$$h_0 \approx \alpha + (1-\alpha)\frac{B_e^*}{B^*}$$

for the case when there is no twist ($\mu = 0$). In the limit of a vanishing seed field ($B_e^* \approx 0$), the tube is now vertical and straight with its boundary lying immediately adjacent to that of its neighbours. Hence, at this and higher heights, the concept of individual fluxtubes has lost its meaning.

Even excluding the merging there are big differences between this approach and that of similarity theories such as those of Schlüter and Temesvary (1958), Yun (1971), Solanki (1982), and Osherovich et al. (1983). These differences are in the field distribution with radius and the treatment of the temperature, and they are related to the force balance in the axial direction. Similarity solutions constrain the radial form of the field and pressure. When this is done, then for a given vertical temperature structure the radial force balance can be satisfied exactly, but axial force balance can be achieved point by point for only *one particular horizontal temperature distribution*. In our approach, we specify the temperature arbitrarily (or through an energy equation) and determine the radial variation of field and pressure, which incidently will be shown to be *not* self-similar, to satisfy both radial and axial force balance simultaneously. We think this has distinct advantages since the temperature can be determined either empirically or through the incorporation of an energy equation into the framework of the theory, which can be done quite easily. Similarity contradicts the use of this equation in any form.

For specifying the external gas pressure, we will employ the HSRASP (Chapman, 1979) model, which combines the HSRA (Gingerich et al., 1971) with a downwards extension obtained from Spruit's (1974) convection zone model. We choose our reference level, $y = 0$ at the $\tau_{5000} = 1$ level of that model.

The actual numerical integration of Eq. (30) is carried out using the backward differentiation formula technique (cf. Gear, 1971), which is an implicit multistep method. In order to carry out the integration we must specify h_0 and h_0' at $y = 0$. h_0 equals unity there by definition and h_0' is adjusted so as to make h_0 smoothly approach a constant value (given by the filling factor α) at large distances.[3] Moreover, as we proceed to deeper and deeper layers for $y < 0$, we expect h_0 to approach the thin fluxtube solution to a closer and closer degree. This means that, wherever we choose our reference level to lie, the degree of depth in the physical atmosphere must be reflected in a relationship between the reference values on the right-hand-side of Eq. (30). If the internal temperature is identical to the external temperature then, the deeper the reference level, the closer the right-hand-side initially must be to zero. This amounts to a relationship between P^*, B^*, P_e^*, B_e^*, and μ which is

$$\Psi = 8\pi(P^* - P_e^*) - B_e^{*2} + (1-\mu)B^{*2} \approx 0 \tag{34}$$

if the reference level lies deep enough down in the atmosphere. Ψ is not *identically* zero because of radial variations in the base conditions. In practice, we here use Eq. (34) to determine P^*.

[3] It can be shown that, unless h_0' has one specific value at the origin, the solution will diverge to either $+\infty$ or 0 at a finite value of y

The small difference in Ψ from zero is a weak function of a^* and is adjusted until a solution is found which is well behaved as y increases in the negative direction.

3. Discussion of results

We will begin this section by ignoring the effects of twist and treat that subject separately in Sect. 3.3. If radiative coupling between the tube and its surroundings is efficient, we might expect the temperature inside the tube to be close to the temperature outside and fairly uniform across the cross-section. For the most part, we shall use this consideration here for determining $p_0(\sigma_0)$ and neglect σ_2 and higher order terms in the temperature. However, later we shall investigate some solutions in which the internal temperature differs from that outside. For example, it is of interest to investigate models in which the internal temperature is lower than that outside, at equal *geometric* height, as suggested by the theoretical model results of Deinzer et al. (1984b). If the internal and external temperatures are equal then, as long as Eq. (34) is satisfied, the solution of Eq. (30), in the limit of a vanishing seed field, is independent of the value B^* and is determined only by the values of the initial radius, a^*, and the filling factor, α.

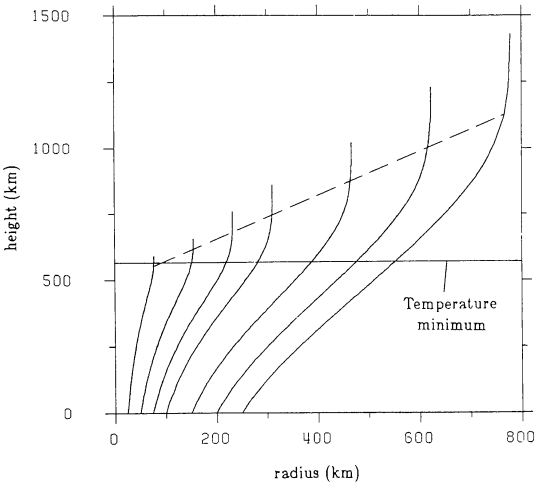

Fig. 3. Height variation of cross-section for different initial base diameters and a filling factor of 0.1. Here, larger base diameters correspond to fewer fluxtubes per unit volume. The horizontal line is the level of the temperature minimum and the dashed curve is the locus of the merging heights. Note that this curve is almost a straight line

3.1. Cross-section and merging height

Figure 2 shows the variation of cross-section with height for different values of the seed field strength. We have taken the base pressure in the tube here to be uniform so that $p_2 = 0$. The initial radius is chosen to be 100 km and the filling factor 0.1. This filling factor lies between the lower values for network fields in quiet regions and the higher values corresponding to strong plages (Solanki and Stenflo, 1984). The value for the radius is close to that given by Muller and Keil (1983) for facular points in continuum observations of the quiet sun network. Since the pressure is uniform across the cross-section here, the calculated fields are potential. As expected, the smaller the seed field strength, the closer the tube expands towards its theoretical limit $R_m = \sqrt{\frac{1}{\alpha}}\, R^*$. Note that, as the seed field becomes very small, the solution becomes essentially independent of its magnitude. Since the tubes merge asymptotically, we consider them merged when h_0'/h_0 (a measure of how vertical the field is) declines to some arbitrary, small value. In practice, we choose this value as 0.05. The merging height defined in this way appears to be approximately independent of the seed field strength.

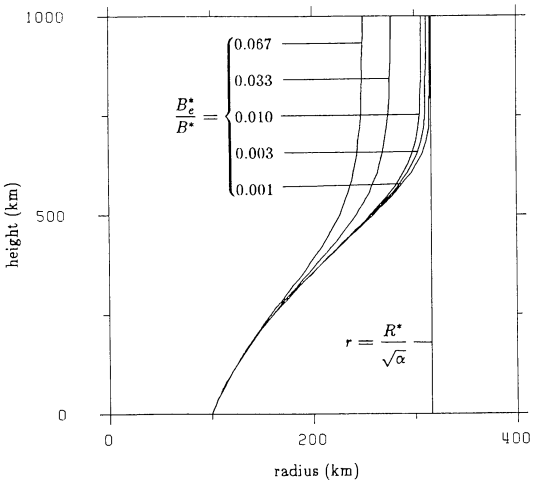

Fig. 2. Variation of the fluxtube cross-section with height for different values of the ratio of seed field strength (B_e^*) to the internal field strength (B^*). We have chosen an initial radius (R^*) of 100 km and a filling factor (α) of 0.1. The vertical line represents the radius for complete merging. We see that, as the seed field strength becomes vanishingly small, the solution becomes essentially independent of its magnitude. Also, the merging height is almost independent of the seed field strength

Spruit and Zwaan (1981) find that, in active regions, small fluxtubes exhibit a broad range of diameters ranging from below their best resolution up to 1.6″ (fluxtubes larger than this are seen as pores). We have therefore also studied the effect of fluxtube diameter on the merging height, although we have concentrated mostly on the so called facular elements, which according to Spruit and Zwaan (1981) have diameters $<0.5''$. The cross-section variation and merging height for different values of R^* but a fixed filling factor of 10% is shown in Fig. 3. The dashed curve represents the locus of merging heights which, curiously, is essentially a linear function of R_m and, hence R^*. Since the filling factor is fixed, a larger value of R^* corresponds to fewer fluxtubes per unit surface area on the Sun. We see then that, the larger the fluxtubes, the higher the level above $\tau_{5000} = 1$ that they merge. The horizontal line in the figure represents the temperature minimum level of the HSRA which we shall consider to be the base of the chromosphere. Hence, unless the tubes are very thin ($R^* < 25$ km), merging takes place in the chromosphere for this filling factor.

A crude expression for the dependence of the merging height on the relevant physical parameters can be obtained by combining the conservation of magnetic flux with the thin fluxtube approximation in an isothermal external atmosphere (Spruit,

1983). This yields

$$z_m = -H \ln \alpha \tag{35}$$

where z_m is the merging height and H the isothermal scale height. Thus, according to Eq. (35), the merging height should be independent of R^*. Fig. 3 shows, however, that this is clearly not the case indicating that field line curvature effects have a significant influence on the merging height.

In Fig. 4, we fix the fluxtube radius to be 100 km and vary the filling factor from 0.025 up to 1.0. As expected, the merging height (indicated by the dashed curve) varies inversely with filling factor. The shape of this curve is approximately logarithmic in accordance with that predicted by Eq. (35), but the constant of proportionality between z_m and $\ln \alpha$ does not correspond to the appropriate scale height. For $\alpha < 0.1$ corresponding to network fields, the merging takes place in the chromosphere. In strong plages, however, the filling factor can be considerably larger and merging can occur in the photosphere. Stenflo and Harvey (1985) have studied the properties of fluxtubes as a function of magnetic flux ($\sim$amplitude of Stokes V). Since the field strength in small fluxtubes appears to be almost independent of flux, the latter quantity is simply proportional to the filling factor. If we take their relationship between α and the maximum Stokes V amplitude of the Fe I 5250.2 Å line: $\alpha = 7.6 V_{\max, 5250}$ and apply this to their point with largest Stokes V amplitude we get a filling factor approaching 40%. This value is corrected for a presumed factor of 2 calibration error in the polarisation of the McMath telescope. The line weakening according to Stenflo (1975) is taken into account but not the effects of the difference in temperature structure between active region and quiet network fluxtubes (Solanki and Stenflo, 1984; Solanki, 1984).

If we no longer constrain the temperature in the tube to be equal to that outside, the merging height then depends upon the value of B^*. Suppose the internal and external temperatures differ by a constant factor over the height range of the HSRASP model. In Fig. 5, we show the dependence of merging height upon the ratio of external (T_e) to internal (T_i) temperatures for three different values of B^*.[4] For $T_e/T_i < 1$, the merging height increases with increasing B^* whereas, for $T_e/T_i > 1$, the reverse is true. The reasons for this behaviour are the following. For $T_e/T_i < 1$, the internal gas pressure falls off more slowly with height than the external gas pressure and, at some height they become nearly equal. Here, the internal magnetic field must become small in order to satisfy the boundary conditions and the cross-section then becomes large enough to ensure merging. Since Eq. (34) must be satisfied at the reference level, the internal pressure, P^*, has to be lower for larger field strengths, B^*. This means that the height at which the internal gas pressure becomes larger than the external gas pressure increases with increasing B^* resulting in a correspondingly higher merging height. Due to the presence of the seed field term in Eq. (30), which dominates over the pressure terms near the merging height, valid solutions can be obtained even above the level at which the internal gas pressure becomes larger than the external gas pressure. Due to magnetic tension the fluxtubes do not become straight suddenly at this height, so that the merging height (defined in Sect. 3.1) can lie above this level. The lines in Fig. 5 are drawn dashed for small T_e/T_i since the low merging height and the related very rapid expansion of the tube lead the model to the limit of its validity. For $T_e/T_i > 1$, on the other hand, the internal pressure falls so rapidly with respect to the external pressure that it soon becomes unimportant. Now, the internal magnetic pressure dominates and produces more rapid expansion and quicker merging as the field strength is increased. Note that, as T_i becomes very small compared to T_e, the merging height approaches an asymptotic value independent of T_i. This is because the internal gas pressure now decreases so rapidly with height that it becomes totally unimportant not far above the reference level.

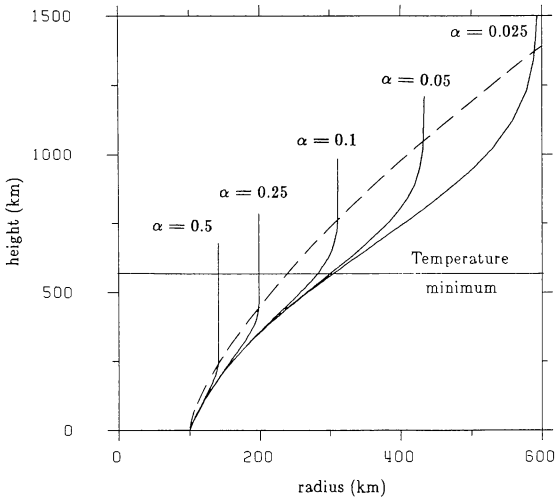

Fig. 4. Variation with height of the cross-section for a fixed base radius of 100 km and different values of the filling factor. As in Fig. 3, the dashed curve represents the locus of the merging heights

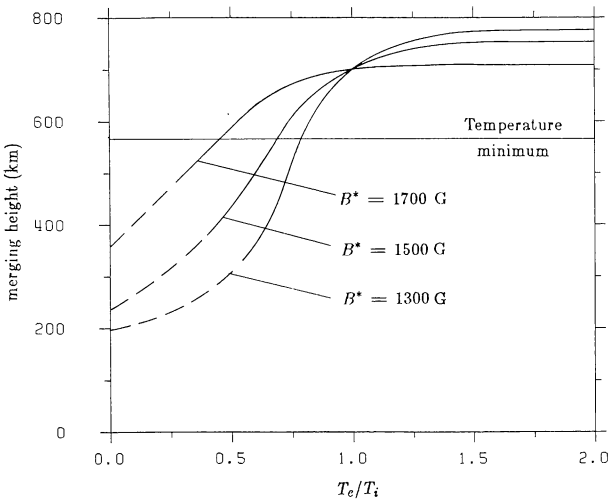

Fig. 5. Dependence of merging height upon ratio of external (T_e) to internal (T_i) temperature for different base magnetic field strengths. At $T_e/T_i = 1$, the merging height is independent of the field strength. For $T_e/T_i > 1$ the height decreases with increasing field strength and for $T_e/T_i < 1$ the reverse is true

[4] Since we are fixing T_e by the HSRASP model atmosphere, the variations in T_e/T_i reflect changes in T_i only

3.2. *Internal structure*

Figure 6 shows the variation of B_z and B_r across the tube at different heights in the atmosphere for a uniform base pressure ($P_2^* = 0$). The heights shown here are incremented in 100 km intervals upwards from the reference level. We see that, at low heights, B_z is almost uniform, in line with that expected from the thin fluxtube approximation. As we proceed upward, the axial field becomes more nonuniform declining outward from the center of the tube. Then, near the merging height, it becomes more uniform again and is, of course, constant after merging. This variation of B_z with radius and height is clearly *not* self-similar. Note that the correction terms to h_0 and f_1 (x^2h_2 and x^3f_3) are not large but also certainly not negligible.

In Fig. 7 we show an example where the pressure at the base is not uniform but increases outward from the center of the tube, i.e., $a^{*2}p_2^* = 1$. The field behaves in a similar way at large distances from the reference level but is distinctly much more nonuniform near $y = 0$. This is because an outward magnetic pressure gradient is needed to balance the imposed inward gas pressure gradient at the lower boundary. As opposed to the variation of the magnetic field quantities, the gas pressure does behave self-similarly if the temperature inside the tube is the same as that outside. This can be seen by using Eqs. (24) and (27) to write the expression for the total pressure for the case of a horizontally uniform temperature ($\sigma_2 = 0$),

$$p = p_0 + x^2 p_2 + \cdots = (1 + x^2 p_2^* h_0) \exp\left(-\int_0^y \frac{dy}{\sigma_0}\right)$$

But, from Eq. (22) we have $h_0 = (a^*/a)^2$, so

$$p \approx \left(1 + p_2^* a^{*2} \left(\frac{x}{a}\right)^2\right) \exp\left(-\int_0^y \frac{dy}{\sigma_0}\right)$$

Obviously, this is a singular case since the self-similar property disappears if the internal and external temperatures are unequal or if the internal temperature varies with x. The above equation shows that the lateral pressure gradient persists even after the fluxtubes have merged. This means that the magnetic field cannot be exactly uniform after merging. But the pressure is declining exponentially and this nonuniformity damps out rapidly as can be seen in the figure.

The case where the pressure at the lower boundary decreases with radius ($a^{*2}p_2 = -1$) is shown in Fig. 8. The result is as expected with the axial magnetic field now increasing outward in the lower part of the tube in order to provide the required inward magnetic pressure gradient. Higher up, the solution is

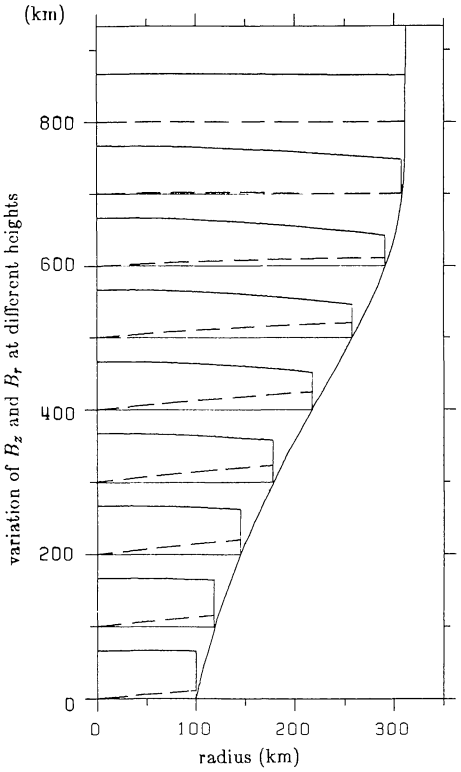

Fig. 6. Radial variation of B_z and B_r at different heights for a typical fluxtube of initial radius equal to 100 km and a filling factor of 0.1. For this case, the base gas pressure is taken to be uniform. To interpret this figure and others like it properly, visualize the figure of the overall fluxtube geometry to be subdivided into groups of subfigures placed at different heights in the tube. Each subfigure contains three curves. At the bottom is a horizontal line defining the height. Above it is the radial variation of B_r shown dashed and, above that, the variation of B_z (solid). As in all figures of this type, both B_z and B_r are normalized to the value of B_z on the axis. Here, the axial field at the base is essentially uniform but then begins to decline outward as the height increases. But, near the merging height, it approaches uniformity again consistent with a uniform vertical cross-section

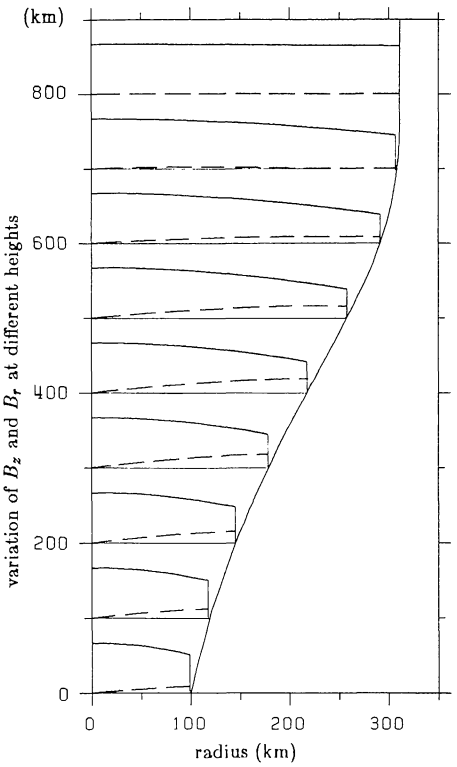

Fig. 7. The same as Fig. 6 but with a base gas pressure increasing outward from the axis. Now, the axial field is no longer uniform at the base since its pressure gradient must now balance the inward gas pressure gradient. At large heights, however, the gas pressure is no longer important and the field approaches uniformity as in Fig. 6

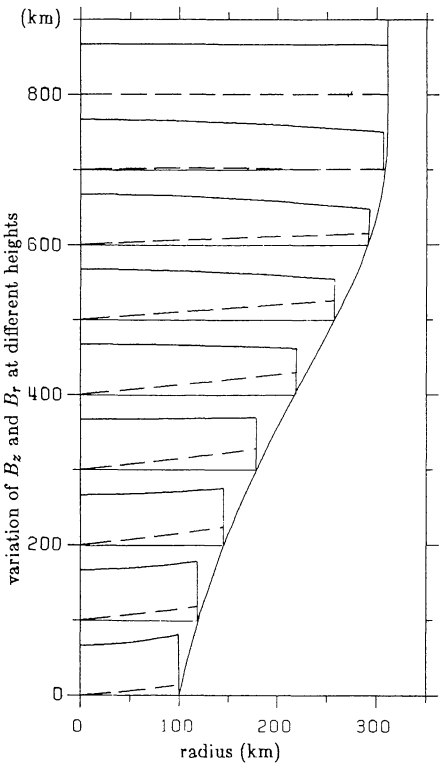

Fig. 8. The same as Fig. 6 but with the base gas pressure now decreasing outward. As expected, the axial field at the base now increases outward to counterbalance the outward gas pressure gradient but then begins to decline outward as the influence of the pressure declines. Eventually, as in the previous cases, the field becomes uniform near the merging height.

similar to the other cases. The similarity of all three solutions in the higher reaches of the tube is due to the rapid decline in gas pressure so that the fields there have essentially forgotten the distribution of pressure at the base.

3.3. *Effects of twist*

Because the higher order terms in the expansion become quite large if the twist is too significant, it is safe within the context of the expansion method we are using to investigate only relatively small values of the initial twist. Nevertheless, several interesting results do emerge from the investigation of even quite small pitch angles. For initial pitch angles less than 15°, the twist has only a small effect upon the cross-section and merging height, the calculation to second order showing a slight decrease in the cross-section at greater heights as compared to the untwisted case. However, we believe this result could be spurious for the following reason: As can be seen from Eq. (30), the net effect of B_θ (in the terms containing μ) is of the same sign as the external pressure and tends to enhance the axial field at the axis, h_0, in agreement with the results of Parker (1974). However, the flux condition correct to second order, Eq. (22), contains only $h_0 a^2$ and not the fourth order term in the axial field $h_2 a^4$. Because h_0 is enhanced, the final calculated cross-section from Eq. (29) will be underestimated without the inclusion of the fourth order term which can become significant at great heights where, in this case, the radial gradient of B_z becomes large. Therefore, our finding from the second order expansion that the cross-section is slightly decreased should not necessarily be taken as a contradiction to the contrary results of Parker (1974, 1976)[5]. It may merely show the inadequacies of a second order expansion when the twist becomes large (as it does near the merging height). In any case, the effect on the cross-section is expected to be quite limited due to the restrictions imposed by merging. We feel that, despite this problem, some qualitative conclusions on twisted tubes can still be reached.

Since, to first order, the pitch angle of the field, η_1, is given by

$$\eta_1 = \tan^{-1}\frac{B_\theta}{B_z} = \tan^{-1} g_1^* a$$

we see that the twist increases with height as the fluxtube broadens in accordance with the results of Parker (1974). Moreover, the number of turns per unit length along the tube remains approximately constant, i.e.,

$$N \sim \frac{1}{a}\tan\eta \approx \text{const.}$$

Figure 9 shows a plot of the tangent of the pitch angle as a function of height for three values of the initial twist. These curves are calculated correct to second order, i.e.,

$$\eta = \tan^{-1}\frac{g_1 a + g_3 a^3}{h_0 + h_2 a^2} \tag{36}$$

As mentioned previously, we see that the twist initially increases strongly with height. However, when the fields begin to merge, the pitch reaches a maximum and then begins to decrease to an

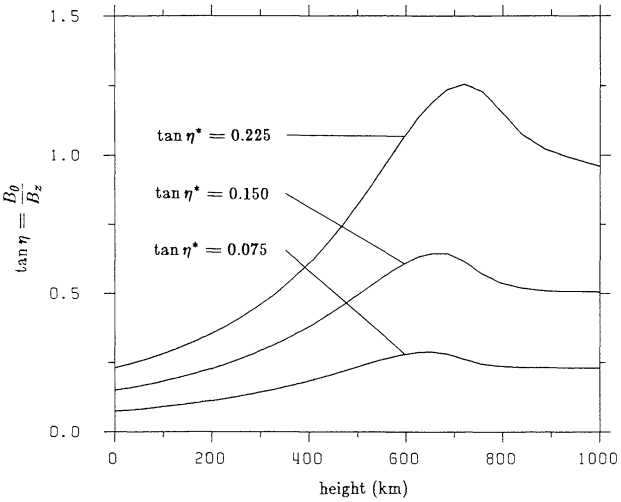

Fig. 9. Variation of pitch angle with height for a twisted fluxtube for different values of the initial twist at the the base. For all these tubes, $R^* = 100$ km and $\alpha = 0.1$. We see that the twist increases strongly with height. But, near the merging height, it reaches a maximum and then declines to a constant value

[5] Although, our analysis is quite different from that of Parker (1974, 1976) in that we specifically include the radial component, B_r, in our treatment

asymptotic constant value. This decrease is due to the second order terms in Eq. (36), primarily the decrease of h_2 (which is negative) as the axial field becomes more uniform at and above the merging height. The constant asymptotic twist at large heights is, of course, consistent with a constant fluxtube radius. Its value is given approximately by

$$\tan\eta_1 \approx \frac{1}{\sqrt{\alpha}} \tan\eta^*$$

where η^* is the initial pitch angle at the surface and η_1 the final value after merging. This result must be viewed with caution since our assumption of cylindrical symmetry breaks down in these regions. Also, it is only approximate since, for twisted tubes, h_2 does not become zero above the merging height (cf. Fig. 10).

Figure 10 shows the variation of B_z and B_θ across the tube cross-section at different heights. We begin at the base with $B_\theta \ll B_z$ but, consistent with Fig. 9, the azimuthal field at great heights eventually dominates at the surface. This azimuthal field produces an inward magnetic pressure force which must be balanced by an outward magnetic pressure force from the axial field (since the lateral gas pressure gradient in this solution is zero). Hence, we find that, with increasing height, the axial field strength declines outward from the tube center correspondingly more rapidly. As opposed to the case shown in Figs. 6, 7, and 8, the axial field here remains nonuniform at all heights – even after merging.

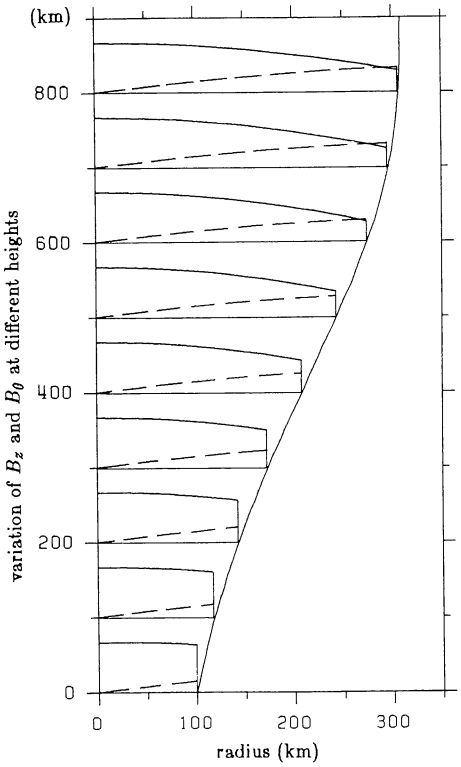

Fig. 10. Radial variation of B_θ (dashed) and B_z (solid) at different heights for $\tan\eta^* = 0.225$, $R^* = 100$ km, and $\alpha = 0.1$. This figure reflects the same properties as in Fig. 9 showing the strong increase in twist with height

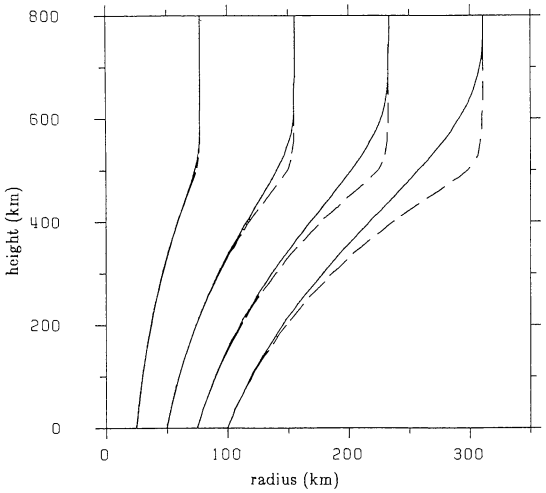

Fig. 11. Comparison of fluxtube cross-section obtained from our expansion technique carried to second order with the thin fluxtube approximation (dashed) also modified through the use of a seed field. The figure shows that the thin fluxtube approximation is quite good near the base but that the deviations from our model become more and more marked as the height increases

3.4. Departures from the thin fluxtube solutions and significance of higher order terms

In Fig. 11, we compare the differences in cross-section for our second order solutions from those obtained using the thin-fluxtube approximation, also modified by the use of a seed field. We use our 'standard' model here (temperature inside and outside equal, pressure laterally uniform, $\alpha = 0.1$) and show tubes with base radii of 25, 50, 75, and 100 km respectively. The differences between the two approximations increase with increasing height and are largest in the vicinity of the merging height. Our solutions show merging at a greater height, due to decreased expansion of the tube, as expected from the presence of magnetic tension. This effect increases with increasing radius (cf. Sect. 3.1). For the thin fluxtube model, the merging height is practically independent of fluxtube radius in accordance with the approximate results of Spruit (1983).

In order to estimate the validity of our expansion technique in general, we show in Fig. 12 plots of the second order and fourth order terms in the expansion of the axial magnetic field strength at the boundary, normalized to its value on the axis, i.e.,

$$\frac{b_z}{h_0} = 1 + \frac{h_2}{h_0} a^2 + \frac{h_4}{h_0} a^4$$

Again this plot corresponds to the 'standard' model with $\alpha = 0.1$, $R^* = 100$ km, no twist, and with the temperature and pressure uniform over the cross-section. For this case, Eqs. (18), (23), and (28) yield simply

$$p_4 = 0$$

$$h_2 = -\frac{1}{4} h_0''$$

$$h_4 = -\frac{1}{16} h_2'' = \frac{1}{64} h_0^{(\mathrm{IV})}$$

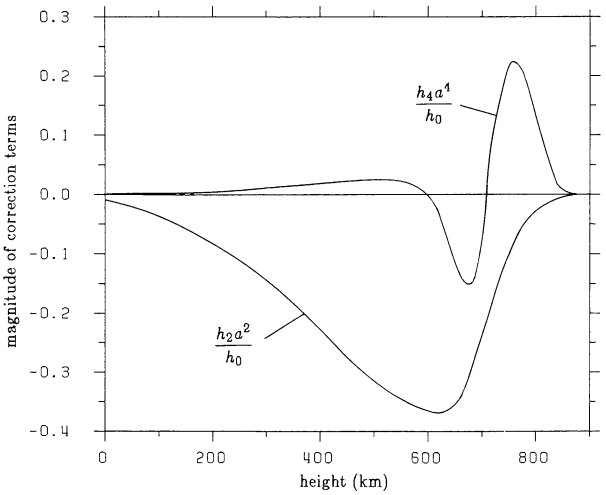

Fig. 12. Variation of the second and fourth order terms in the expansion for B_z with height. The curves show the ratio of these terms to the zeroth order terms. The second order term grows with height and actually becomes significant near the merging height but then drops quickly to zero. The fourth order term is very small at low heights but also increases near the height where the fields merge. This figure corresponds to our "standard" model with $R^* = 100$ km and $\alpha = 0.1$. For fluxtubes thinner than this, these terms should become correspondingly smaller

We see that both the second and fourth order terms are small near the base but the second order term grows with height until just below the merging height (at about 750 km) when it quickly drops to zero. The fourth order term, which is proportional to the curvature of the second order term, remains quite small until merging begins to occur where it begins to reflect the adjustment of h_2 towards zero. p_4 and h_4 remain small for most of the models studied by us, including those with $p_2 \neq 0$. h_4 may, however, become large for tubes with large twist. Of course, for a thinner fluxtube than this, the correction terms should become correspondingly smaller.

4. Summary and conclusions

In this paper we have constructed a fluxtube model with two major goals in mind. One was to treat the tube within the context of a collection of similar tubes, which may or may not be twisted, so that merging of the tubes as they expand with height must be considered. The second goal was to examine higher order departures from the thin fluxtube models to obtain information on the effects of magnetic field curvature and other higher order effects upon the tube structure and merging properties without restricting ourselves to similarity theory. The similarity models cannot treat arbitrary temperature distributions across the cross-section and also places severe restrictions upon the internal structure. To accomplish these goals we chose to use an expansion technique in which the appropriate variables such as magnetic field strength, gas pressure, and temperature are expanded in power series in the radial variable perpendicular to the tube axis and then solve the appropriate MHD equations for the height variation of the various coefficients by equating equal powers in the equations to any ascending order of accuracy desired. If this process is carried out to second order, one ultimately obtains a nonlinear second order differential equation for the magnetic field along the tube's axis which must be solved numerically.

In order to treat the merging of the tubes with each other conveniently, we chose to specify a small 'seed' field existing between the fluxtubes to simulate the presence of neighbouring tubes. This seed field is used for mathematical convenience and has no effect upon the solution for merging height, structure, etc., as long as its magnitude is small as compared to that of the field in the tube. The use of this field external to the tubes allows them to merge smoothly as expected physically.

For all our models, we specified the external atmosphere by the HSRASP (Chapman, 1979). The reference level where the boundary conditions are applied was taken at $\tau_{5000} = 1$ of that model. For most cases we chose the internal temperature to be uniform across the tube and, assuming efficient radiative coupling, equal to the external temperature at all heights. We also chose the base gas pressure to be uniform. For these conditions, the solution for an untwisted tube is independent of the magnetic field strength at the base and is a function only of the initial radius and filling factor. For a fixed filling factor, the merging height is essentially a linearly increasing function of radius (for a fixed filling factor, increased radius corresponds to fewer fluxtubes per unit area) and, for tubes greater in diameter than about 25 km, merging takes place in the chromosphere for filling factors of 0.1 or less. For a fixed fluxtube diameter, on the other hand, the merging height varies inversely with filling factor as expected.

If the internal temperature is no longer constrained to be equal to that outside, then the solution does depend upon field strength. If the internal temperature exceeds that outside, the merging height increases with increasing field strength whereas, if it is less, the reverse is true. As discussed in the text, this behaviour reflects the difference in the decline of the internal and external gas pressures due to the different scale heights in the two regions.

In general, we find that the thin fluxtube solution is quite good low in the atmosphere as we might expect but, as the tubes expand, the deviations soon become apparent with the greatest departures occuring near the merging height. Our solution shows that the effects of magnetic field line curvature extends the merging to greater heights than predicted by the thin fluxtube approximation modified by the use of a seed field. But the departures are not so enormous, that we can say that this approximation can be a useful tool for many applications.

Turning now to the internal structure of the tube, if the base gas pressure is uniform, then the axial field at the base is also uniform but then begins to decline outward from the axis more and more markedly as the fluxtube expands upward. But near the height where merging occurs, the axial field again tends towards uniformity consistent with a vertical fluxtube of constant cross-section. If the base pressure increases outward from the axis, then the base axial field strength decreases correspondingly so that the outward magnetic pressure gradient can balance the inward gas pressure gradient (the curvature has little influence at this height). However, the axial field again approaches uniformity as the tube merge. If, on the other hand, the base gas pressure decreases outward from the axis, the reverse is true with the axial field strength initially increasing outward.

At this point it is necessary to point out that, for all our solutions the variation of the magnetic field distribution with height is *decidedly not self-similar*. The gas pressure distribution,

however, does behave self-similarly with height, but only when the internal temperature is uniform and also equal to the external temperature. Self-similar solutions require one specific temperature distribution with radius in order to satisfy force balance in both directions, even though an energy equation is not used. Here, we are specifying the temperature distribution independently so that self-similarity should not be expected. We think this is a decided advantage since, in principle, an energy equation could easily be incorporated into our formalism.

For a twisted fluxtube, the higher order terms in our expansion become significant if the initial twist is too large and our formalism cannot really be trusted. However, we feel we can safely discuss some physical implications of slightly twisted fields. For the cases we consider, the twist does not have a large effect on the overall cross-section and merging height. In accordance with the results of Parker (1974), the pitch angle increases strongly with height since the number of turns per unit length remains approximately constant while the cross-section increases rapidly. However, as the fields begin to merge, the pitch angle reaches a maximum and then begins to decrease towards a constant asymptotic value consistent with a constant cross-section. Though the azimuthal field at the surface is small as compared to the axial component there at the base, it eventually dominates at great heights. This produces a strong inward magnetic pressure gradient and curvature force which must be balanced by an outward magnetic pressure force due to the axial field (since the gas pressure at these heights is small). Hence, the axial field must decrease outward from the axis and continues to do so even after merging. Presumably, after merging, fields of opposite polarity will come in contact with each other resulting in magnetic reconnection which could serve to combine tubes integrally with their neighbours (Parker, 1983).

It is generally agreed that the magnetic field of unipolar regions expands until it comes into contact with field lines coming from neighbouring regions. Different theoretical models have been proposed for this expansion (e.g. Gabriel, 1976; Anzer and Galloway, 1983b). The results from these models have been interpreted to give "canopy heights" of around 1500 km above the photosphere in quiet regions, where "canopy height" is interpreted as the height at which the atmosphere begins to be dominated by the magnetic field. On the other hand Giovanelli (1980), Giovanelli and Jones (1982), and Jones and Giovanelli (1983) have found evidence from magnetograph recordings for magnetic canopies lying between 500 and 800 km in the atmosphere, near both active and quiet network regions. Here canopies are regions of magnetic field lying over non-magnetic regions. If their interpretation of the observations is correct, then we should expect on the basis of our analysis that the individual fluxtubes would not be fully merged when the canopy begins to form, i.e. when the fields become strongly inclined. Consequently, there clearly is a need to study the structure and merging of non-vertical fluxtubes.

In conclusion, we think the present model offers distinct advantages over the thin fluxtube approach since it does elucidate the effects of field line curvature, nonuniformities in the internal structure, and merging properties due to the presence of neighbouring tubes. Although we only carry our analysis through terms of second order in radius this approach, in principle, can be carried out to higher orders of accuracy if so desired. However, the numerical complexity increases enormously. In the meantime, we hope that the present model will be useful for empirical modeling of such structures in the solar atmosphere. Ultimately, however, exact MHD solutions for this problem are certainly feasible. This has been demonstrated, for example, by the time-dependent relaxation technique employed by Endler (1971), Steinolfson et al. (1982), and Suess (1983) for the coronal streamer problem and by Deinzer et al. (1984a,b) for fluxtubes in slab geometry. An equally promising method would be the iterative method used by Pneuman and Kopp (1971) for streamers, which has recently been applied to sunspots by Pizzo (1985).

Acknowledgments. One of us (GWP) wishes to thank the Institut für Astronomie, Zürich and its director J.O. Stenflo for their hospitality during his visit there. Another of us (SKS) gratefully acknowledges the helpful discussions with B. Roberts on some mathematical aspects of the solution of Eq. (30).

References

Anzer, U., Galloway, D.J.: 1983a, in *Solar and Stellar Magnetic Fields: Origins and Coronal Effects*, J.O. Stenflo (Ed.), IAU *Symp.* **102**, 339
Anzer, U., Galloway, D.J.: 1983b, *Monthly Notices Roy. Astron. Soc.* **203**, 637
Browning, P.K., Priest, E.R.: 1983, *Astrophys. J.* **266**, 848
Chapman, G.A.: 1979, *Astrophys. J.* **232**, 923
Defouw, R.J.: 1976, *Astrophys. J.* **209**, 266
Deinzer, W., Hensler, G., Schüssler, M., Weisshaar, E.: 1984a, *Astron. Astrophys.* **139**, 426
Deinzer, W., Hensler, G., Schüssler, M., Weisshaar, E.: 1984b, *Astron. Astrophys.* **139**, 435
Endler, F.: 1971, PhD Thesis, Göttingen University
Ferraro, V.C.A., Plumpton, C.: 1966, *An Introduction to Magneto-Fluid Mechanics*, Clarendon Press Oxford
Gabriel A.H.: 1976, *Phil. Trans. Roy. Soc. London* **A281**, 339
Gear, C.W.: 1971, *Numerical Initial Value Problems in Ordinary Differential Equations*, Prentice Hall
Gingerich, O., Noyes, R.W., Kalkofen, W., Cuny, Y.: 1971, *Solar Phys.* **18**, 347
Giovanelli, R.G.: 1980, *Solar Phys.* **68**, 49
Giovanelli, R.G., Jones, H.P.: 1982, *Solar Phys.* **79**, 267
Harvey, J.W.: 1977, in *Highlights of Astronomy*, E.A. Müller (Ed.), Vol. 4, Part **II**, 223
Howard, R., Stenflo, J.O.: 1972, *Solar Phys.* **22**, 402
Jones, H.P., Giovanelli, R.G.: 1983, *Solar Phys.* **87**, 37
Meyer, E., Schmitt, H.U., Simon, G.W., Weiss, N.O.: 1979, *Astron. Astrophys.* **76**, 35
Muller, R., Keil, S.L.: 1983, *Solar Phys.* **87**, 243
Osherovich, V.A. Flå, T., Chapman, G.A.: 1983, *Astrophys. J.* **286**, 412
Parker, E.N.: 1974, *Astrophys. J.* **191**, 245
Parker, E.N.: 1976, *Astrophys. Space Sci.* **44**, 107
Parker, E.N.: 1983, *Astrophys. J.* **264**, 635
Pizzo, V.J.: 1985, *Astrophys. J.* (in press)
Pneuman, G.W., Kopp, R.A.: 1971, *Solar Phys.* **18**, 258
Roberts, B., Webb, A.R.: 1978, *Solar Phys.* **56**, 5
Schlüter, A., Temesvary, S.: 1958, *Electromagnetic Phenomena in Cosmical physics, IAU Symp.* **6**, 263
Simon, G.W., Weiss, N.O., Nye, A.: 1983, *Solar Phys.* **87**, 65
Solanki, S.K.: 1982, Diplomarbeit, ETH Zürich
Solanki, S.K.: 1984, *Proceedings of the Fourth European Meeting*

on Solar Physics – 'The Hydromagnetics of the Sun,' ESA **SP-220**, 63
Solanki, S.K., Stenflo, J.O.: 1984, *Astron. Astrophys.* **140**, 185
Spruit, H.C.: 1974, *Solar Phys.* **34**, 277
Spruit, H.C.: 1976, *Solar Phys.* **50**, 269
Spruit, H.C.: 1981, in S. Jordan (Ed.) *The Sun as a Star*, NASA **SP-450**, 385
Spruit, H.C.: 1983, in *Solar and Stellar Magnetic Fields: Origins and Coronal Effects*, J.O. Stenflo (Ed.), IAU *Symp.* **102**, 41
Spruit, H.C., Zwaan, C.: 1981, *Solar Phys.* **70**, 207
Steinolfson, R.S., Suess, S.T., Wu, S.T.: 1982, *Astrophys. J.* **255**, 730
Stenflo, J.O.: 1973, *Solar Phys.* **32**, 41
Stenflo, J.O.: 1975, *Solar Phys.* **42**, 79
Stenflo, J.O., Harvey, J.W.: 1985, *Solar Phys.* **95**, 99
Suess, S.T.: 1983, *NASA Cont. Publ.*, NASA **CP-2280**, 183
Unno, W., Ribes, E.: 1979, *Astron. Astrophys.* **73**, 314
Wilson, P.R.: 1977a, *Astrophys. J.* **214**, 611
Wilson, P.R.: 1977b, *Astrophys. J.* **214**, 917
Yun, H.S.: 1971, *Solar Phys.* **16**, 398